Journal of the European Ceramic Society **13** (1994) 387–394

V_2O_5, Nb_2O_5 and Ta_2O_5 Doped Zirconia Ceramics

G. Gritzner* & C. Puchner

Institut für Chemische Technologie Anorganischer Stoffe, Johannes Kepler Universität Linz, A-4045 Linz, Austria

(Received 2 June 1993; revised version received 11 October 1993; accepted 29 November 1993)

Abstract

V_2O_5, Nb_2O_5 and Ta_2O_5 doped zirconia ceramics were made from precursors prepared by hydrolysis of the respective metal alkoxide solutions in 1-propanol with water. The amorphous, coprecipitated hydroxides were calcined at 900°C. Oxidic zirconia powders doped with 5 and 15 mol.% V_2O_5 as well as powders with 1, 2, 5, 7, 10, 12, 15, 17 and 20 mol.% Nb_2O_5 and Ta_2O_5, respectively, were isostatically compacted and subjected to different sintering conditions. The powders were characterized by the specific surface areas, the particle size distributions and by electron microscopy. Powders calcined at 1400°C with more than 12 mol.% Nb_2O_5 and Ta_2O_5, respectively were found to be orthorhombic. Powders with lower contents of Nb_2O_5 and Ta_2O_5, consisted of mixtures of the monoclinic and the orthorhombic phase. Increases in the doping oxides led to increases in the b- and c-axes accompanied by a decrease in the a-axis. V_2O_5 doped powders and sintered samples were monoclinic.

The powders doped with Nb_2O_5 or Ta_2O_5 were sintered at temperatures ranging from 1500 to 1650°C. Three-point bend strengths, Weibull moduli, fracture toughnesses, Vickers hardnesses, densities and phase compositions were measured for the sintered specimens. Average three-point bend strengths for samples consisting of the pure orthorhombic phase ranged between 134 and 181 MPa, samples with both monoclinic and orthorhombic phases yielded lower bend strengths. Fracture toughnesses were around 3 MPa $m^{1/2}$, Vickers hardnesses between 2·3 and 9·7 GPa. Theoretical densities between 96·8 and 99·7% were observed. No phase transformations occurred during fracture.

Die Ausgangspulver zur Herstellung von V_2O_5, Nb_2O_5 und Ta_2O_5 dotierter Zirkoniumdioxid-Keramik wurden durch Hydrolyse der Lösungen der entsprechenden Metallalkoxide in 1-Propanol hergestellt. Die amorphen Hydroxide wurden bei 900°C kalziniert. Die Pulver wurden durch Bestimmung der spezifischen Oberflächen und der Partikelgrößenverteilungen charakterisiert sowie elektronenmikroskopisch untersucht. Pulver mit 5 und 15 mol.% V_2O_5, sowie mit jeweils 1, 2, 5, 7, 10, 12, 15, 17 und 20 mol.% Nb_2O_5 bzw. Ta_2O_5 wurden nach dem Attritieren isostatisch verpreßt und gesintert. Pulver mit mehr als 12 mol.% Nb_2O_5 bzw. Ta_2O_5 bestanden nur aus der orthorhombischen Phase. Pulver mit geringeren Gehalten an Dotieroxiden bildeten ein Gemisch aus der orthorhombischen und der monoklinen Phase. Die b und c Gitterparameter nahmen mit zunehmenden Gehalten an Dotieroxiden zu, der a Gitterparameter leicht ab. V_2O_5 dotierte Pulver sowie die daraus hergestellten Sinterkörper waren monoklin.

Die mit Nb_2O_5 bzw. Ta_2O_5 dotierten Pulver wurden bei Temperaturen zwischen 1500°C und 1650°C gesintert. Von den gesinterten Keramiken wurden Dreipunktbiegefestigkeiten, Weibull Moduli, Bruchzähigkeiten, Vickershärten, Dichten und Phasenzusammensetzungen ermittelt. Die Mittelwerte der Dreipunktbiegefestigkeiten lagen für Proben, die nur aus der orthorhombischen Phase bestanden, zwischen 134 und 181 MPa. Sinterkörper, die sowohl die orthorhombische wie auch die monokline Phase enthielten, hatten deutlich geringere Biegebruchfestigkeiten. Die Bruchzähigkeiten betrugen rund 3 MPa $m^{1/2}$. Die Vickershärten lagen zwischen 2·3 und 9·7 GPa, die theoretischen Dichten zwischen 96·8 und 99·7%. Während des Bruchs der Keramiken kam es zu keinen Phasenumwandlungen.

Des céramiques à base de zircone dopée au V_2O_5, Nb_2O_5 et Ta_2O_5 ont été élaborées à partir de précurseurs préparés par hydrolyse de solutions d'alcoolates dans du 1-propanol avec de l'eau. Les hydroxydes coprécipités amorphes ont été calcinés à 900°C. Les poudres de zircone dopées avec 5 et 15% en mole de V_2O_5 et celles dopées avec 1, 2, 5, 7, 10, 12, 15, 17 et 20% en mole de Nb_2O_5 et Ta_2O_5 ont été pressées isostatiquement et frittées sous différentes conditions. La surface spécifique et la

* To whom correspondence should be addressed.

Journal of the European Ceramic Society 0955-2219/94/$7.00

distribution granulométrique ont été déterminées pour toutes les poudres et un examen par microscopie électronique a permis de compléter la caractérisation. Les poudres calcinées à 1400°C contenant des taux de Nb_2O_5 et Ta_2O_5 supérieurs à 12% en mole se caractérisent par une phase orthorhombique tandis que les poudres ayant des teneurs plus faibles en Nb_2O_5 et Ta_2O_5 sont constituées d'un mélange de phases monoclinique et orthorhombique. L'augmentation de la teneur en oxydes dopants entraine une augmentation des axes b et c et une diminution de l'axe a. Les poudres dopées au V_2O_5 ainsi que les échantillons frittés sont monocliniques.

Les poudres dopées avec Nb_2O_5 et Ta_2O_5 ont été frittées à des températures de l'ordre de 1500 à 1650°C. Les propriétés suivantes ont été mesurées pour tous les matériaux frittés: résistance en flexion 3 points, module de Weibull, ténacité, dureté Vickers, densité et composition cristallographiques. Les valeurs moyennes de résistance en flexion 3 points pour les matériaux constitués par une phase orthorhombique pure se situent entre 134 et 181 MPa, les matériaux contenant les phases monoclinique et orthorhombique présentent des résistances en flexion plus faibles. Les ténacités sont de l'ordre de 3 MPa $m^{1/2}$, les duretés Vickers entre 2·3 et 9·7 GPa et les densités théoriques entre 96·8 et 99·7 %.

Aucune transformation n'a été observée durant la rupture.

1 Introduction

Zirconia exhibits polymorphy, it is monoclinic up to 1170°C, tetragonal until 2370°C and above this temperature cubic (fluorite structure). The high-temperature phases can either be stabilized or maintained in metastable form at room temperature by doping with various oxides. Both fully and partially stabilized zirconias are of considerable technical interest. The stress-induced martensitic transformation of metastable tetragonal zirconia into the monoclinic phase forms the basis for transformation-toughened zirconia. Besides these three phases an orthorhombic or possibly two orthorhombic phases (connutite and distorted fluorite structure) have been observed under high pressures and temperatures[1–8] or as a metastable phase upon quenching.[9] The existence of an orthorhombic phase has also been found in transmission electron microscopy studies in thin foils of yttria[10] or magnesia doped zirconia[11,12] as well as during stress-induced transformations of partially stabilized zirconia.[13,14] Neutron diffraction and thermodilatometry studies on magnesia partially stabilized zirconia confirmed that most of the tetragonal zirconia transformed to the orthorhombic phase when cooled to 30 K.[15] $6ZrO_2 . Nb_2O_5$ and $6ZrO_2 . Ta_2O_5$ were found to have orthorhombic symmetry.[4,16] Powders of Nb_2O_5-doped zirconia have been prepared and their sintering behaviour as well as the analysis of the sintered bodies by mercury porosimetry, densities and by scanning electron microscopy of the fracture surfaces have been reported.[17] Very little information, however, is presently available on the sintering behaviour and the mechanical properties of orthorhombic zirconia. Thus we started investigations on vanadia, niobia and tantala doped zirconia to obtain the orthorhombic phase and to study the sintering behaviour and the mechanical properties of such ceramics.

2 Experimental Procedure

2.1 Apparatus and testing

BET surface area measurements were carried out on a Quantasorb (Quantachrome, USA). Crystallite sizes were calculated from $d = 6/(\rho A_s)$ where d is the crystallite diameter, ρ the density and A_s the specific surface area. The particle size distribution was analysed by means of a laser particle sizer (Coulter LS 130, USA).

X-ray diffraction spectra were measured on a Geigerflex D/max II with Ni-filtered CuK_α radiation (Rigaku, Japan) between 25 and 80° (40 kV, 20 mA) with Si (99·999 %, Balzers, Liechtenstein) as internal standard. The powders for the analysis of the lattice parameters were heated to 1000°C at a rate of 5 K min^{-1}, then to 1400°C at 3 K min^{-1}. The cooling rate was 20 K min^{-1}. The powders were then mixed with Si (3 : 1). X-ray fluorescence analysis was performed on a Geigerflex M 3064 spectrometer with a Rh anode (Rigaku, Japan) with 35 kV and 15 mA. Electron micrographs were obtained on a JSM-6400 scanning microscope (Jeol, Japan). Thermogravimetric measurements were carried out on a TG-770 (Stanton Redcraft, UK). A HT 64/17 oven (Naber, Germany) with a maximum temperature of 1750°C served for sintering.

The sintered samples were polished on diamond discs (220 and 600) and then with diamond powder (6 μm and 3 μm) to specimen of 4 mm × 3 mm × 40 mm. The edges of the tensile surfaces were chamfered prior to testing. Three-point bend-strengths were measured on these samples with a 20 mm span. The load was increased at a rate of 12 N s^{-1}. Vickers hardnesses were obtained under a load of 49 N. K_{Ic} values were calculated from the indentation method[18] from 10 good indents employing the following relation:[19] $K_{Ic} = 0{\cdot}0824\ P/c^{1.5}$ (K_{Ic} in MPa $m^{1/2}$, P in MN, c in m).[20]

Density measurements were performed employing the Archimedes principle, the results are given as averages for five samples. Porous samples were covered with zapon lacquer, first dried at 50°C to avoid bubble formation and then overnight at 100°C. The samples were either chemically etched in 60 wt.% NaOH for 2 h at 180°C or thermally etched at 1450°C for 1–2 h. Rather stringent conditions for etching were necessary, since these ceramics are quite corrosion resistant. Lattice parameters were obtained from powders calcined at 1400°C. The percentage of orthorhombic phase was calculated from the peak areas of the orthorhombic (111) and the monoclinic (111) peaks following a procedure published for tetragonal and monoclinic zirconia.[21]

2.2 Powder preparation and sintering

Zirconium-1-propoxide was commercially available (Johnson Matthey, USA). 1-Propanol was dried by adding 5 g of magnesium turnings and some iodine per litre of the solvent. Upon refluxing for 5 h the solvent was distilled. The 1-propoxides of niobium and tantalum were prepared following published methods.[21,22] $TaCl_5$ and $NbCl_5$ (Johnson Matthey) were dissolved in benzene under vigorous stirring. Benzene was refluxed over calcium hydride prior to use. The stoichiometric amount of 1-propanol was added and the solution was cooled in an ice bath. Ammonia, dried over $CaCl_2$, was added under constant cooling of the mixture. Following the separation and washing of the precipitated ammonium chloride with propanol, the remaining benzene and 1-propanol in the filtrate were evaporated at 60°C and 2000 Pa. The products were purified by vacuum distillation. Niobiumpenta-1-propoxide was distilled between 185 and 189°C at 532 Pa (yield: 76% theory), tantalum penta-1-propoxide between 203 and 207°C at 667 Pa (yield: 98% theory).

Solutions of the alkoxides in 1-propanol were prepared in a glove-box under the exclusion of moisture to avoid premature hydrolysis. The solutions of the metal alkoxides were sprayed into water. The suspensions of the precipitated hydroxides were stirred for 1 h. The precipitates were filtered, first washed with water and then with ethanol. The powders were dried at 70°C and 667 Pa. Powders containing Ta_2O_5 and Nb_2O_5 were calcined for 2 h at 900°C (heating rate 5 K min^{-1}), those containing V_2O_5 for 6 h at 500°C. Calcined Ta_2O_5 and Nb_2O_5 doped powders were white, V_2O_5 doped powders were green. Portions of 30–36 g of the calcined oxides were attrition milled with 1200 g of yttria stabilized zirconia balls (2 mm diameter, 600 min^{-1}) in 160 ml of 1-propanol for 4 h. Upon filtering off the balls through a 1 mm sieve, the solvent was evaporated under vacuum and the powders dried at 100°C at 667 Pa. Polyethylene from the attritor was burned out at 600°C.

The powders were isostatically compressed at 800 bar into blocks of 20 mm × 15 mm × 48 mm. These blocks were presintered at 1000°C. Specimens of 5 mm × 4 mm × 40 mm were cut on the blocks and polished. These samples were then sintered at a rate of 1 K min^{-1} up to 400°C and kept there for 1 h. The temperature was then increased at 5 K min^{-1} to 1000°C and at 3 K min^{-1} to the final sintering temperature. The final sintering temperature was maintained for 2 h. The samples were then cooled at 20 K min^{-1}.

3 Results and Discussion

3.1 Properties of powders and sintered specimen

All precipitated hydroxides were amorphous. Thermogravimetric studies on the coprecipitates showed that the conversion to the oxides was complete around 700°C (Fig. 1). The particle size distributions for the calcined powders were rather inhomogeneous with agglomerates up to 150 μm necessitating attrition milling. After attrition particle size distributions from below 0·1 μm up to 18 μm, with N_{50} values below 1·3 μm were

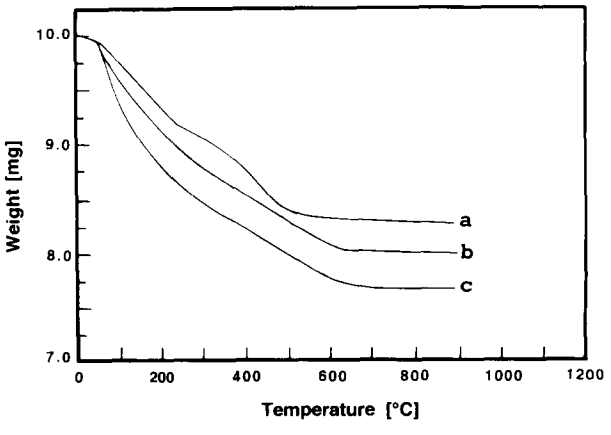

Fig. 1. Thermogravimetry of coprecipitated hydroxides: (a) 5 mol.% V_2O_5; (b) 5 mol.% Ta_2O_5; (c) 5 mol.% Nb_2O_5.

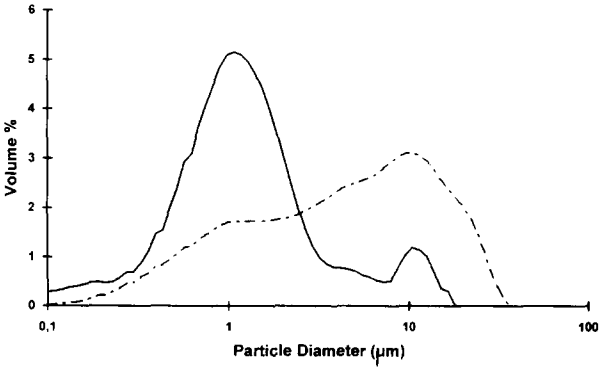

Fig. 2. Particle size distribution of calcined (dashed line) and attrited zirconia (solid line) doped with 5 mol.% Nb_2O_5.

Table 1. Properties of Nb_2O_5-doped zirconia

Mol. % Nb_2O_5	*Specific surface area[a] ($m^2\ g^{-1}$)*	*Green densities ($g\ cm^{-3}$)*	*Crystallite size[a] (nm)*	*Densities*			
				1500°C	*1550°C*	*1600°C*	*1650°C*
1	29·6 (3)	2·443 (2)	33	—[b]	—[b]	—[b]	—[b]
2	27·0 (1)	2·552 (3)	37	5·320 (3)	5·323 (10)	5·285 (8)	5·182 (2)
5	26·4 (1)	2·664 (1)	37	5·559 (7)	5·636 (3)	5·818 (15)	5·340 (2)
7	24·2 (1)	2·693 (1)	41	5·199 (4)	5·755 (6)	5·901 (8)	5·972 (5)
10	22·2 (2)	2·802 (2)	44	4·472 (4)	5·877 (10)	6·068 (9)	5·897 (3)
12	22·4 (1)	2·878 (9)	44	5·824 (3)	5·930 (9)	6·082 (8)	6·098 (6)
15	21·1 (3)	2·914 (7)	46	6·034 (2)	5·982 (14)	6·070 (11)	6·036 (4)
17	21·0 (1)	3·028 (6)	46	6·034 (9)	5·960 (6)	6·072 (7)	5·820 (16)
20	19·9 (2)	3·067 (2)	49	5·883 (14)	5·780 (7)	5·634 (12)	5·517 (8)

[a] Attrited powder.
[b] Cracked after sintering.

found (Fig. 2). The specific surface areas and the densities of the calcined, attrited powders are summarized in Tables 1 and 2. The specific surface areas of the attrited powders decreased from 30 to 20 $m^2\ g^{-1}$ for 1–20 mol.% Nb_2O_5, the specific surface areas for Ta_2O_5 (1–20 mol.%) increased from 24 to 37 $m^2\ g^{-1}$ with increasing concentration of the dopant. The sizes of the crystallites calculated from the specific surface areas ranged from 25 to 50 nm, in close agreement with observations made by scanning electron microscopy (Fig. 3). Green densities increased with increasing concentrations of Nb_2O_5 or Ta_2O_5. Preliminary experiments on densities as a function of the sintering temperatures were carried out on zirconia doped with 10 mol.% Nb_2O_5 and 10 mol.% Ta_2O_5 in the temperature range from 1200°C to 1700°C (Table 3). The densities of Nb_2O_5-doped zirconia generally increased up to sintering temperatures of 1600°C followed by a slight decrease at higher temperatures. The highest densities for Ta_2O_5-doped zirconia were found at 1650°C. Based on these results sintering temperatures of 1600°C were used for Nb_2O_5-doped zirconia and of 1650°C for Ta_2O_5-doped zirconia. The sintered bodies were white to light beige in colour. The mechanical properties of the Nb_2O_5-doped and Ta_2O_5-doped zirconia, respectively, are summarized in Tables 4 and 5. Average three-point bend strengths for orthorhombic samples ranged from 130 to 180 MPa. These values are somewhat lower than three-point bend strengths observed for CeO_2-doped[23] and Y_2O_3—CeO_2[24,25] codoped tetragonal zirconia but higher than for fully stabilized cubic zirconia.[26] The considerably smaller values for bend strengths compared to Y_2O_3-stabilized tetragonal zirconias are due to the absence of any transformation-toughening during crack propagation. The smaller bend strengths for the mixed monoclinic-orthorhombic zirconia samples are due to a partial o/m transformation upon cooling accompanied by a volume change and crack formation. The Nb_2O_5-doped and Ta_2O_5-doped zirconia were very brittle. Studies on the fracture surfaces showed that the cracks initiated on pores at or very close to the tensile surface. The fractures were transcrystalline for purely orthorhombic samples, but intercrystalline for mixed orthorhombic-monoclinic specimens (Fig. 4). Scanning electron micrographs of the microstructure showed elongated crystallites between 1 and 3 μm (Fig. 5). Weibull moduli for Ta_2O_5 stabilized zirconia were generally greater than for

Table 2. Properties of Ta_2O_5-doped zirconia

Mol. % Ta_2O_5	*Specific surface area[a] ($m^2\ g^{-1}$)*	*Green densities ($g\ cm^{-3}$)*	*Crystallite size[a] (nm)*	*Densities after sintering*			
				1500°C	*1550°C*	*1600°C*	*1650°C*
1	24·0 (1)	2·448 (4)	40	5·491 (6)	5·462 (9)	5·399 (9)	5·449 (1)
2	26·8 (4)	2·545 (7)	36	5·687 (2)	5·695 (2)	5·666 (7)	5·669 (2)
5	30·4 (1)	2·665 (3)	30	5·934 (6)	5·873 (4)	5·871 (6)	5·851 (1)
7	32·4 (1)	2·733 (9)	28	6·078 (4)	6·098 (3)	6·032 (11)	6·011 (3)
10	33·9 (3)	2·841 (4)	39	5·920 (4)	6·302 (15)	6·776 (5)	6·882 (13)
12	33·3 (1)	3·222 (7)	26	6·811 (8)	6·935 (6)	6·985 (30)	7·009 (11)
15	32·5 (4)	3·062 (2)	25	6·911 (9)	6·935 (8)	6·981 (8)	7·133 (4)
17	33·8 (1)	3·045 (6)	24	6·920 (7)	7·001 (5)	7·114 (7)	7·269 (9)
20	36·7 (2)	3·134 (6)	21	6·957 (11)	7·095 (6)	7·269 (11)	7·384 (6)

[a] Attrited powders.

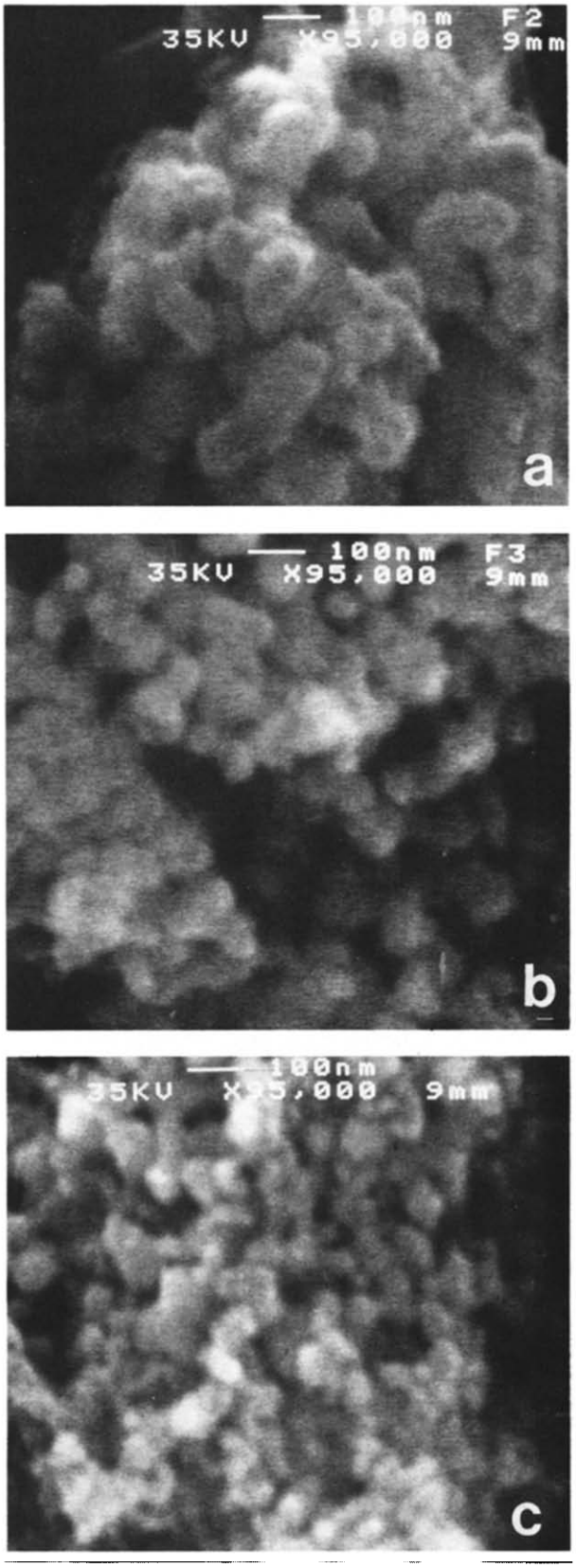

Fig. 3. Scanning electron micrograph of doped zirconia powders: (a) 2 mol.% Nb_2O_5; (b) 12 mol.% Nb_2O_5; (c) 20 mol.% Ta_2O_5.

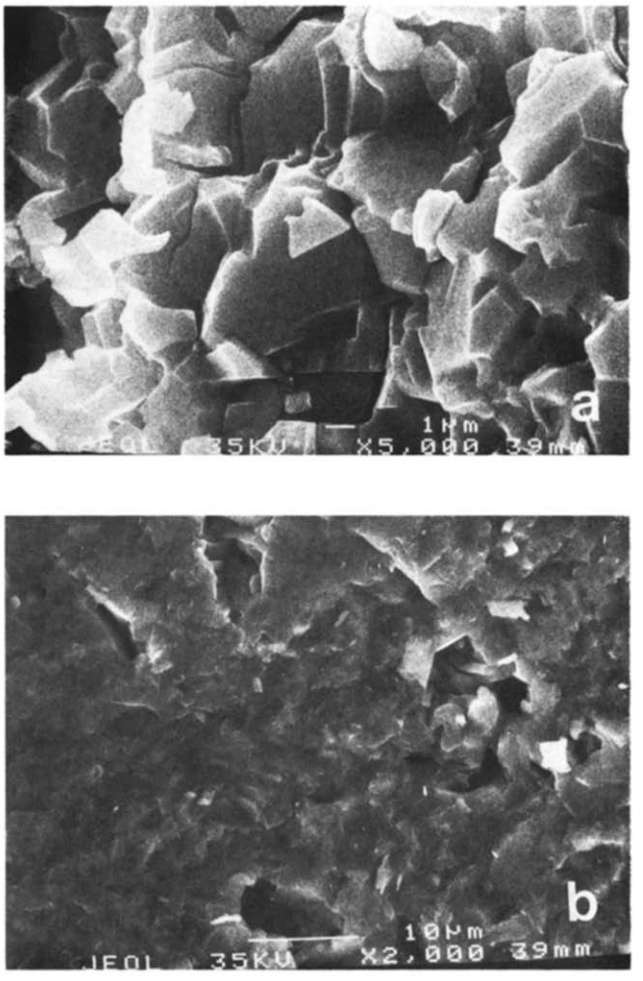

Fig. 4. Fracture surface of doped zirconia: (a) 5 mol.% Ta_2O_5, 50% orthorhombic phase; (b) 12 mol.% Nb_2O_5-doped zirconia, pure orthorhombic phase.

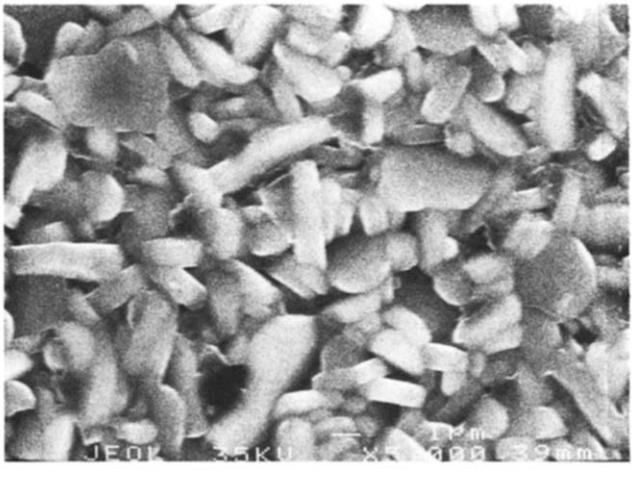

Fig. 5. Microstructure of zirconia doped with 15 mol.% Nb_2O_5 (pure orthorhombic phase).

Nb_2O_5-doped zirconia. High concentrations of doping oxides resulted in lower Weibull moduli and thus in a considerable scatter for the data for three-point bend strengths. The Vickers hardness of Nb_2O_5-doped zirconia showed a maximum of 9·3 GPa around 12 mol.%, whereas the Vickers hardness for Ta_2O_5-doped zirconia increased with increasing Ta_2O_5 content up to 9·7 GPa at 17 mol.%. Again Vickers hardness were comparable to or somewhat lower than the values for Y_2O_3 doped, CeO_2-doped or Y_2O_3–CeO_2-codoped tetragonal zirconia.

Table 3. Densities as a function of the sintering temperatures

Sintering temperature (°C)	*10 mol.% Nb_2O_5*		*10 mol.% Ta_2O_5*	
	Density (g cm^{-3})	*Th. density (%)*	*Density (g cm^{-3})*	*Th. density (%)*
1200	3·121 (3)	51·02	4·008 (2)	58·08
1300	3·245 (1)	53·05	4·635 (2)	67·16
1400	3·461 (2)	56·58	5·160 (2)	74·77
1500	4·472 (4)	73·10	5·920 (4)	85·78
1550	5·877 (10)	96·07	6·302 (15)	91·31
1600	6·068 (9)	99·19	6·776 (5)	98·18
1650	5·897 (3)	96·40	6·882 (13)	99·72
1700	5·409 (22)	88·42	6·765 (13)	98·03

Table 4. Mechanical properties of Nb_2O_5-doped zirconia sintered at 1600°C

Mol.% Nb_2O_5	*σ_{3P}[a] MPa*		*m[b]*	*HV[c] (GPa)*	*K_{Ic} (MPa m$^{1/2}$)*	*ρ[d] (g cm^{-3})*	*Rel. density (%)*	*Orthorh. phase (%)*
	Aver.	*Max.*						
7	[e]	[e]	[e]	3·8 ± 0·2	[f]	5·972	98·0	46
10	54 ± 11	60	5·2	6·5 ± 0·4	[f]	6·068	99·2	87
12	150 ± 24	182	7·0	9·4 ± 1·3	2·9 ± 0·4	6·098	99·5	100
15	179 ± 28	233	7·0	6·5 ± 0·8	3·0 ± 0·5	6·070	98·7	100
17	181 ± 43	278	4·3	7·0 ± 0·8	3·1 ± 0·8	6·072	98·6	100
20[g]	—	—		6·5 ± 0·6	3·3 ± 0·4	5·974	96·7	100

[a] Three point bend strength.
[b] Weibull modulus.
[c] Vickers hardness.
[d] Density.
[e] Cracked samples.
[f] Indentations could not be evaluated.
[g] Sintered at 1450°C.

Table 5. Mechanical properties of Ta_2O_5 doped zirconia sintered at 1650°C

Mol.% Ta_2O_5	*σ_{3P}[a] MPa*		*m[b]*	*HV[c] (GPa)*	*K_{Ic} (MPa m$^{1/2}$)*	*ρ[d] (g cm^{-3})*	*Rel. density (%)*	*Orthorh. phase (%)*
	Aver.	*Max.*						
5	[e]	[e]	[e]	[f]	[g]	[e]		50
7	[e]	[e]	[e]	2·3 ± 0·3	[g]	[e]		68
10	99 ± 7	110	16·2	4·0 ± 0·4	[g]	6·882	99·7	91
12	134 ± 11	144	14·0	8·6 ± 0·4	3·1 ± 0·2	7·008	99·3	100
15	162 ± 26	200	6·6	8·6 ± 0·3	3·1 ± 0·4	7·133	98·0	100
17	189 ± 25	216	8·3	9·7 ± 0·1	2·8 ± 0·4	7·269	98·0	100
20	138 ± 40	180	2·8	9·4 ± 0·9	3·0 ± 0·6	7·384	96·8	100

[a] Three point bend strength.
[b] Weibull modulus.
[c] Vickers hardness.
[d] Density.
[e] Cracked samples.
[f] Indentations could not be evaluated.
[g] Crack length could not be measured.

Table 6. Lattice parameters and theoretical densities for Nb_2O_5 and Ta_2O_5 stabilized zirconia

Mol.%	*Nb_2O_5 stabilized*				*Ta_2O_5 stabilized*			
	a (nm)	*b (nm)*	*c (nm)*	*Th. density (g cm^{-3})*	*a (nm)*	*b (nm)*	*c (nm)*	*Th. density (g cm^{-3})*
0[a]	0·5042	0·5092	0·5257	6·062	0·5042	0·5092	0·5257	6·062
5	0·5010	0·5115	0·5290	6·082	0·5024	0·5122	0·5291	6·487
7	0·5012	0·5129	0·5294	6·097	0·5018	0·5125	0·5293	6·658
10	0·5003	0·5126	0·5295	6·117	0·5000	0·5125	0·5293	6·901
12	0·4990	0·5137	0·5306	6·130	0·4992	0·5133	0·5303	7·057
15	0·4964	0·5154	0·5312	6·149	0·4969	0·5150	0·5305	7·279
17	0·4951	0·5153	0·5307	6·161	0·4957	0·5146	0·5300	7·422
20	0·4956	0·5160	0·5312	6·178	0·4957	0·5156	0·5308	7·626

[a] Ref. 27.

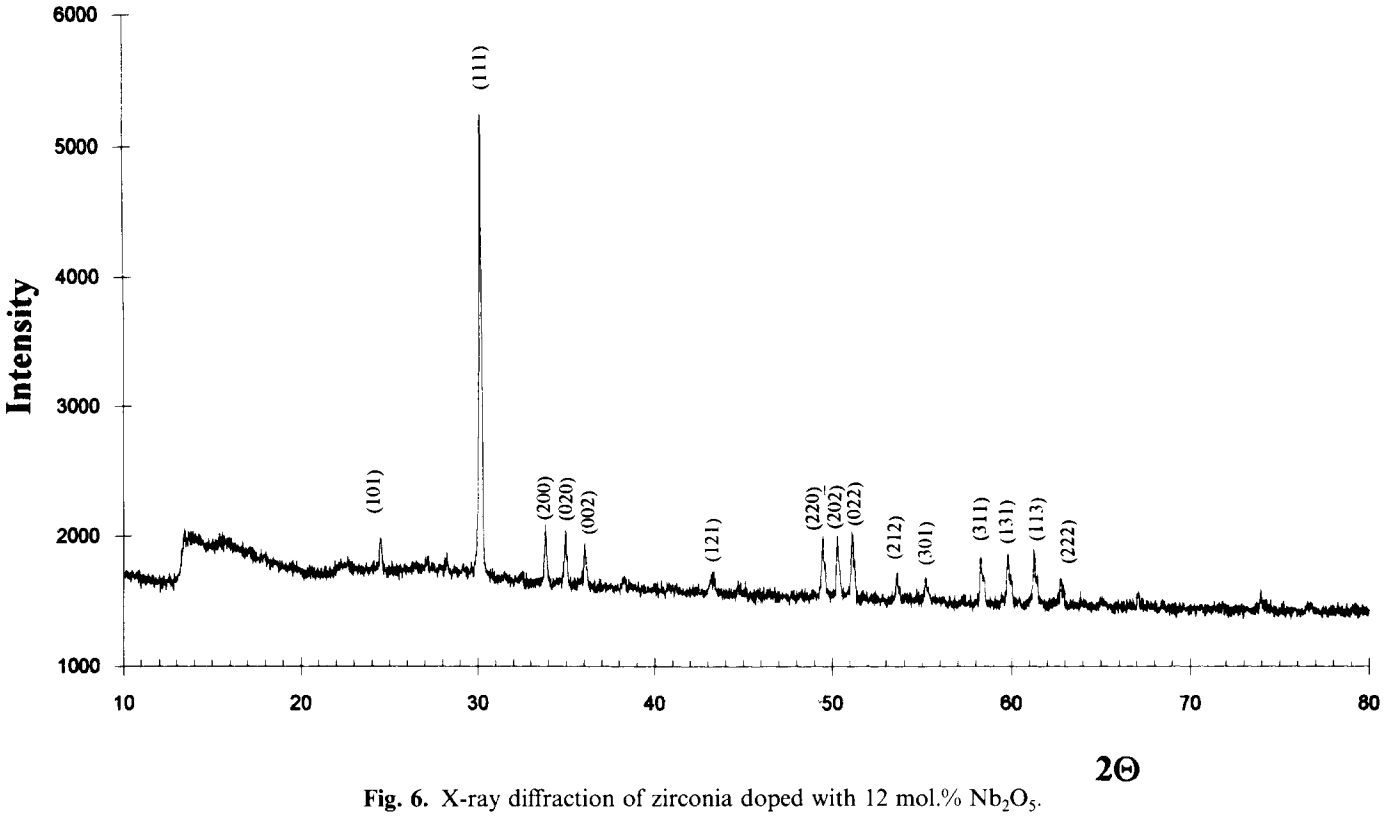

Fig. 6. X-ray diffraction of zirconia doped with 12 mol.% Nb_2O_5.

Zirconia doped with V_2O_5 was monoclinic. Calcined powders had specific surface areas of 79 $m^2\ g^{-1}$ (5 mol.% V_2O_5) and 60 $m^2\ g^{-1}$ (15 mol.% V_2O_5) respectively. Sintered samples cracked upon cooling. Furthermore V_2O_5 reacted with the casing. Therefore no further studies were carried out with this dopant.

3.2 Lattice parameters

Additions of Nb_2O_5 and Ta_2O_5 led to a stabilization of the orthorhombic phase (Fig. 6). Generally a decrease in the a-axis and an increase in the b- and c-axes were observed. Lattice parameters obtained for Nb_2O_5 and Ta_2O_5 are given in Table 6. The changes in the lattice parameters can be presented by the following equations:

$$a = a_o + k_a\ (X_2O_5/\text{mol.}\%),$$
$$b = b_o + k_b\ (X_2O_5/\text{mol.}\%),$$
$$c = c_o + k_c\ (X_2O_5/\text{mol.}\%)$$

The respective values for a_o, b_o, c_o, k_a, k_b and k_c are summarized in Table 7. Theoretical densities for Nb_2O_5 and Ta_2O_5 doped zirconia were obtained from the lattice parameters. The lattice parameters for orthorhombic zirconia were indexed as published for to $6ZrO_2 . Ta_2O_5$.[27]

Table 7. Coefficients for the calculation of lattice parameters of Nb_2O_5 and Ta_2O_5 doped zirconia as a function of the dopant concentration[a]

Oxide	a_o *(nm)*	$10^4\ k_a$	b_0 *(nm)*	$10^4\ k_b$	c_0 *(nm)*	$10^4\ k_c$
Nb_2O_5	0·504(1)	−4·667	0·509(7)	3·361	0·527(0)	2·469
Ta_2O_5	0·504(6)	−4·765	0·509(9)	2·947	0·527(2)	2·036

[a] $a = a_0 + k_a\ (X_2O_5/\text{mol.}\%)$, $b = b_0 + k_b\ (X_2O_5/\text{mol.}\%)$, $c = c_0 + k_c\ (X_2O_5/\text{mol. }\%)$.

4 Conclusions

Zirconia ceramics doped with Nb_2O_5 or Ta_2O_5 above 12 mol.% yielded orthorhombic sintered bodies. The bend strengths and fracture toughnesses for these brittle materials were rather low, since no phase transformation occurred during fracture. Vickers hardnesses were comparable to other zirconia ceramics. The Nb_2O_5 or Ta_2O_5 doped ceramics were quite resistant to corrosion in alkaline and acid media.

Acknowledgements

Financial support by the Fonds zur Förderung der wissenschaftlichen Forschung (Austria) and the Jubiläumsfonds der Österreichischen Nationalbank is gratefully appreciated. The authors thank Mr K. Kellner for carrying out the xrd-measurements and Dipl.-Ing. M. Ratajski for electron micrographs

References

1. Bendeliany, N. A., Popova, S. V. & Vereshchagin, L. P., New high pressure phase of ZrO_2 & HfO_2. *Geokhimiya*, **6** (1967) 683.

2. Roth, R. S. & Coughanour, L. W., Phase equilibrium in the systems, titania–niobia and zirconia–niobia. *J. Res. Nat. Bur. Stand.*, **55** (1955) 209–13.
3. Bocquillon, G. & Susse, C., Phase diagram of zirconia under pressure. *Rev. Int. Hautes Temp. Refract.*, **6** (1969) 263–6.
4. Roth, R. S., Waring, J. L., Brower, W. S. & Parker, H. S., Superstructure of the orthorhombic Nb_2O_5–$6ZrO_2$ type phase(s) in the Nb_2O_5–ZrO_2 and Ta_2O_5–ZrO_2 systems. *Nat. Bur. Stand. Publ.*, **364** (1972) 183–95.
5. Lityagina, L. M., Kabalkina, S. S., Pashkina, T. A. & Khozyainov, A. I., Polymorphism of ZrO_2 at high pressures. *Sov. Phys. Solid State*, **20** (1978) 2009–10.
6. Liu, L. G., New high pressure phase of ZrO_2 and HfO_2. *J. Phys. Chem. Solids*, **41** (1980) 331–4.
7. Block, S., Da Jornada, J. A. H. & Piermarini, G. J., Pressure–temperature phase diagram of zirconia. *J. Am. Ceram. Soc.*, **68** (1985) 497–9.
8. Arashi, H. & Ishigame, M., Raman spectroscopic studies of the polymorphism in ZrO_2 at high pressures. *Phys. Status Solidi (a)*, **71** (1982) 313–21.
9. Suyama, R., Ashida, T. & Kume, S., Synthesis of the orthorhombic phase of ZrO_2. *J. Am. Ceram. Soc.*, **68** (1985) C314–5.
10. Bestgen, H., Chaim, R. & Heuer, A. H., Thin-foil phase transformations of tetragonal ZrO_2 in a ZrO_2-8 wt% Y_2O_3 alloy. *J. Am. Ceram. Soc.*, **71** (1988) 826–31.
11. Kishi, E. H., Howard, C. J. & Hill, R. J., Crystal structure of orthorhombic zirconia in partially stabilized zirconia. *J. Am. Ceram. Soc.*, **72** (1989) 1757–60.
12. Heuer, A. H., Lanteri, V., Farmer, S. C., Chaim, R., Lee, R. R, Kibbel, B. W. & Dickerson, R. M., On the orthorhombic phase in ZrO_2-based alloys. *J. Mater. Sci.*, **24** (1989) 124–32.
13. Lenz, L. K. & Heuer, A. H., Stress-induced transformation during subcritical crack growth in partially stabilized zirconia. *J. Am. Ceram. Soc.*, **65** (1982) C192–4.
14. Heuer, A. H. & Schoenlein, L. H., Thermal shock resistance of Mg-PSZ. *J. Mater. Sci.*, **20** (1985) 3421–7.
15. Howard, C. J., Kisi E. H., Roberts, R. B. & Hill, R. J., Neutron diffraction studies of phase transformations between tetragonal and orthorhombic zirconia in magnesia-partially-stabilized zirconia. *J. Am. Ceram. Soc.*, **73** (1990) 2828–33.
16. Trunov, V. K., Vladimirova, Z. A., Kovba, L. M. & Komissarova, L. N., Double oxides in the ZrO_2–Nb_2O_5 system. *Inorg. Mater.*, **1** (1965) 1055–7.
17. Garcia, D. E., Ove, C. S., Longo, E. & Varela, J. A., Preparation and sintering of niobia-doped zirconia. In *Ceramics Today—Tomorrow's Ceramics, Part B*, ed. P. Vincenzi. Elsevier Science Publishers 1991 pp. 915–24.
18. Anstis, G. R., Chantikul, P., Lawn, B. R. & Marshall, D. B., A critical evaluation of indentation techniques for measuring fracture toughness: I, Direct crack measurement. *J. Am. Ceram. Soc.*, **64** (1981) 522–38.
19. Ponton, C. B. & Rawlings, D., Vickers Indentation fracture toughness test. Part 1. Review of literature and formulation of standardized indentation toughness equations. *Mater. Sci. Technol.*, **5** (1989) 865–72.
20. Evans, P. A., Stevens, R. & Binner J. G. P., Quantitative X-ray diffraction analysis of polymorphic mixes of pure zirconia. *Br. Ceram. Trans. J.*, **83** (1984) 39–43.
21. Bradley, C. D., Wardlaw, W. & Whitley, A., Normal alkoxides of quinquevalent tantalum. *J. Chem. Soc.*, **1** (1955) 726–8.
22. Bradley, C. D., Chakravarti, B. N. & Wardlaw, W., Normal alkoxides of quinquevalent niobium. *J. Chem. Soc.*, **7** (1956) 2381–4.
23. Puchner, C., Kladnig, W. & Gritzner, G., Mechanical properties of CeO_2-doped ZrO_2. *J. Mater. Sci. Lett.*, **9** (1990) 94–96.
24. Spielbüchler, P. & Gritzner, G., Mechanical properties of yttria- and ceria-doped zirconia ceramics. *J. Mater. Sci. Lett.*, **11** (1992) 1426–8.
25. Gritzner, G. & Steger, P., Y_2O_3–CeO_2 doped ZrO_2 ceramics from coprecipitated oxalate precursors. *J. Eur. Ceram. Soc.*, **12** (1993) 461–6.
26. Abraham, I. & Gritzner, G., Mechanical properties of doped cubic zirconia ceramics. *J. Mater. Sci. Lett.* **12** (1993) 795–7.
27. JCPDS-International Centre for Diffraction Data 37-1413.